

# Simulation of uranium mononitride spent fuel: A crystallographic approach.

C. Degueldre<sup>1\*</sup>, D.T. Goddard<sup>2\*\*</sup>, G. Berhane<sup>1</sup>, A. Simpson<sup>3</sup>, C. Boxall<sup>1</sup>,

1. Engineering Department, Lancaster University, LA1 4YW, UK

2. National Nuclear Laboratory, Springfields, Salwick, Preston, Lancashire, PR4 0XJ, UK

3. National Nuclear Laboratory, Central Laboratory, Sellafield, Seascale, Cumbria, CA20 1PG, UK.

[c.degueldre@lancaster.ac.uk](mailto:c.degueldre@lancaster.ac.uk) ;

[dave.t.goddard@uknpl.com](mailto:dave.t.goddard@uknpl.com); [g.berhane@lancaster.ac.uk](mailto:g.berhane@lancaster.ac.uk); [allan.simpson@uknpl.com](mailto:allan.simpson@uknpl.com);

[c.boxall@btinternet.com](mailto:c.boxall@btinternet.com)

## Abstract

Uranium mononitride (UN) is an attractive fuel for a range of reactors, including, with adequate protection against reaction with water, for large scale and small modular light water reactors. The study of the speciation of fission products (Fps) in spent UN fuel is required to understand their properties such as phase stability and retention during long term storage and disposal. The present study reviews and applies Hume-Rothery rules to predict this speciation. This law provides an estimate of the way UN may form solid solutions with actinide (An) and fission product mononitrides from Beginning of Life (BoL) to End of Life (EoL). Composition at EoL is estimated for a high burnup fuel (60 MW d kg<sup>-1</sup>) using the FISPIN fuel inventory code. Many Fps are trivalent (Ln, Y, Zr, Nb) and are expected to recrystallize in face centred cubic (fcc) solid solutions with UN. Other Fps are divalent (Ba, Sr) and monovalent (Cs, Rb) and some elements are non-valent (Mo, Tc, Ru, Rh, Pd) as well as noble gases (Xe, Kr), and halides (I, Br) which may form nano-precipitates. Actinides formed by neutron capture of <sup>238</sup>U are all An<sup>3+</sup> which are also expected and found in fcc solid solution with UN.

The spent fuel is consequently formed of a large fraction of solid soluble nitrides (U, An, Ln, Y, Zr, Nb)N forming a single rather homogeneous phase according to the Hume-Rothery rules. This phase will also follow Vegard's law. Because of the low temperature of the fuel, the Fps are expected to be soluble or nano-dispersed precipitates. Microscopic precipitated phases are not expected.

**Keywords**, uranium mononitride; fission product nitride solubility; actinide nitride solubility; transition metal precipitate; nitride spent fuel.

\*e-mail: \* [c.degueldre@lancaster.ac.uk](mailto:c.degueldre@lancaster.ac.uk) , \*\* [dave.t.goddard@uknpl.com](mailto:dave.t.goddard@uknpl.com)

## 1. Introduction

Uranium mononitride (UN) is attractive as a future fuel for reactors of the fourth generation such as in fast neutron Na, Pb or Pb-Bi nuclear test reactors e.g. Bauer (1972)[1], Ekberg, *et al* (2018)[2]. It is also undergoing consideration for use in thermal spectrum Light Water Reactors (LWRs), Brown, *et al* (2014)[3], with due consideration of its reactivity with water and need for  $^{15}\text{N}$  enrichment. With its high uranium density it is also an attractive fuel for micro-reactor concepts including for space power applications, Matthews, *et al* (1988)[4].

Uranium nitrides exist in three chemical forms the dinitride ( $\text{UN}_2$ ), the sesquinitride ( $\text{U}_2\text{N}_3$ ) and the mononitride (UN). Uranium dinitride ( $\text{UN}_2$ ) decomposes to uranium sesquinitride ( $\text{U}_2\text{N}_3$ ) then to uranium mononitride (UN) as reported by Silva *et al* (2009)[5]. The preparation of dense uranium nitride fuel compacts, with density greater than 90% of theoretical, has been described by Tennery *et al* (1971)[6]. While uranium mononitride has an elevated melting point (as observed by Carvajal Nunez *et al* (2014)[7]), it has been found to decompose below this temperature, Lunev *et al* (2016)[8]. Dissociation of UN was observed to start even at  $1500^\circ\text{C}$ , Inoyue & Leitnaker (1968)[9].

Uranium mononitride is considered superior because of its high fissionable density (see Hayes *et al* (1990)[10]), a thermal conductivity 4-8 times higher than  $\text{UO}_2$ , as reported by Kim & Ahn (2021)[11], resulting in a lower thermal gradient in the fuel sections and less irradiation induced restructuring, revealing consequently low fission gas releases and low reactivity with cladding materials. Although fuel swelling is slightly higher than for  $\text{UO}_2$ , the combined mechanical, thermal (see Takahashi *et al* (1971)[12]) and radiation stability (see Martin *et al* (1965)[13]) of UN makes it a promising alternative to conventional oxide fuel.

However, deployment of this fuel has been restricted by the resistance to sintering and by the difficulty to produce an adequate microstructure, the additional costs induced by  $^{15}\text{N}$  enrichment, as well as the known predisposition to interaction with steam. UN pellets sintered using spark plasma sintering methods have shown how sintering temperature, time, and holding pressure can be used to control grain growth to produce a material with a desirable porosity and grain size, as pointed out by Johnson & Adorno Lopes (2018)[14]. Furthermore, porosity closure was observed at densities of 96% theoretical density, corresponding to a material with enough porosity to accommodate LWR burnup.

The present study focuses on the speciation of fission product and actinides generated during fuel irradiation. After a literature review, an inventory code is used to predict the composition of a spent UN fuel and then rules that dictate the formation of solid solutions in the complex phases that form the spent fuel are considered.

## 2. Literature review on UN: from fuel to spent fuel properties

Baranov, *et al* (2016)[15] investigated the thermal stability of uranium nitride as well as its structure. This fuel material is also very compact thanks to its cubic fcc structure.

Uranium mononitride (UN) has been studied in its inert matrix fuel variant ((Pu,Zr)N) in the early 2000's e.g. Degueldre & Yamashita (2003)[16] to burn excess plutonium in an efficient way. In this fuel the fissile component is Pu and the inert matrix is Zr, both form nitrides chemically. Streit (2004)[17] investigated the fabrication and characterization of (Pu,Zr)N fuels and their analogous compounds (U,Zr)N, (Ce,Zr)N, (Nd,Zr)N and ZrN. They all formed solid solutions that crystallized in the cubic fcc system.

These crystallographic results were confirmed by ab initio modelling of fission products (i.e. Y, Zr, Nb, Ce, Nd, Sm, Eu, Gd, Mo, Ru, Rh, Pd, Sr and Ba) in uranium mononitride assessing their embedding and local contributions to fuel swelling, see Klipfel *et al* (2013)[18]. Fission products (Fps) in uranium mononitride have demonstrated to be first incorporated at U vacancies in bound defects. The local volume changes caused by Fp substitutions have been assessed using Density Functional Theory (DFT) and combined with the Fp concentrations obtained from neutron calculations to predict fission product swelling in UN. The calculated linear swelling of the UN fuel that resulted from these calculations, and the assumption that fission products **do not interact** and **do not form secondary phases**, led to a reasonable estimation for the swelling rate as a function of burn-up (or time).

Post-irradiation examination of a uranium-free nitride fuel, (see Hania *et al* (2015)[19] supported these predictions. Two identical Pu<sub>0.3</sub>Zr<sub>0.7</sub>N fuel segments were irradiated in 1 bar helium in the High Flux Reactor (HFR) Petten at a linear power of 46-47 kW m<sup>-1</sup> at Beginning of Life (BoL) and with an average cladding temperature of 505°C. The pins were irradiated to a plutonium burn-up of 9.7% (88 MW d kg<sup>-1</sup>) in 170 effective full power days. Both pins remained fully intact. The post-irradiation examination showed an overall swelling rate of the fuel to be 0.92 vol-%/%%FIHMA (Fission per Initial Heavy Metal Atom). Fission gas release was 5-6%, while helium release was greater than 50%. No fuel restructuring was observed and only mild cracking. Electron Probe MicroAnalysis (EPMA) showed a fourfold increase in burn-up towards the pellet edge. **All detectable fission products except to some extent the noble metals were found to be evenly distributed within the matrix**, indicating good solubility (see Fig.1). A general conclusion of this investigation was that ZrN has potential to be used as an inert matrix for burning plutonium at high destruction rates.

**Fig. 1:** Pu<sub>0.3</sub>Zr<sub>0.7</sub>N spent fuel Post-irradiation Examination (PIE): Wavelength Dispersive X-ray (WDX) mapping for Nd, Ba and Xe at equal sample positions, revealing a homogeneous distribution of fission products. At the bottom of the images is the fuel-clad interface (CONF-30-L sample). Ref. Hania *et al* (2015) [19] with courtesy Elsevier

Chemical forms of solid fission products in an irradiated (U,Pu)N fuel were described by Arai *et al*, (1994) [20]. They noted that in addition to the matrix phase dissolving zirconium, niobium, yttrium and rare earth elements, two kinds of inclusion were identified. One was an URu<sub>3</sub> type intermetallic compound composed of U and Ru, Rh and Pd. The other was an alloy containing molybdenum metal as the major constituent.

Furthermore, Thetford & Mignanelli (2003) [21] found that in high-temperature tests on (U,Zr)N the actinide mononitrides are stable under nitrogen up to their melting point. A simple rule was established comparing the crystal structure and lattice parameter of the solute nitride, with that of the nitride fuel. Only solute nitrides with the same crystal structure as the fuel were considered soluble and the extent of solubility derived from an assessment of the difference between the room temperature lattice parameters of the solute and solvent nitrides. Complete

solubility was proposed for relative lattice parameter differences between  $-7.5\%$  and  $+8.5\%$  while solubility was negligible for values less than  $-16\%$ .

No nitride phases have been reported for the platinum element group. These elements are expected to precipitate as intermetallic phases, such as  $(U,Pu)Pd_3$  or  $(U,Pu)(Pd,Rh,Ru)_3$  including possibly some Mo and Tc.

Also in spent nitride fuel Se and Te are expected to be found either in elemental form or in compounds with electronegative elements (e.g.  $Cs_2Te$ ).

### 3. Theoretical background

#### 3.1 Nuclide inventory calculations

##### Formalisation

The fission products and actinides inventories of UN spent fuel has been calculated using FISPIN (FISsion Product INventory), the UK spent fuel inventory code, presented originally by Burstall (1979) [22]. FISPIN is distributed by ANSWERS [23]. It can be used for estimating the nuclide inventory of fuel from any modern reactor, including light water and advanced gas cooled reactors, when used in conjunction with suitable reactor neutronics codes such as WIMS, see Newton *et al* (2008) [24]. Inventories at multiple time steps both during and post irradiation can be calculated as well as the impact of downstream separation processes.

The FISPIN solution solves a set of partial differential equations that account for spontaneous decay, fission products and activation products. The mathematical solution based on Rutherford's model, see Rutherford (1911) [25], defining the cross section ( $\sigma$ ) properties which for neutron capture can read:

$$dN/dt = -N \sigma \phi \quad (1)$$

was proposed by Bateman and is described as follows:

$$\frac{dN_i}{dt} = -(\lambda_i + \sigma_i \phi) N_i + \sum_j N_j (\lambda_j^i + \sigma_j^i \phi) + \sum_k N_k \sigma_k^f \phi y_{ki}$$

where  $N_i$  is the number of atoms of isotope  $i$  at time  $t$ ,  $\lambda_i$  is the decay constant of  $i^{\text{th}}$  nuclide,  $\lambda_j^i$  is the decay constant from isotope  $i$  to isotope  $j$ ,  $\phi$  is the neutron flux,  $y_{ki}$  is the independent fission yield of isotope  $i$  from fissile species  $k$ ,  $\sigma_j^i$  is the microscopic fission cross-section of nuclide  $j$  from nuclide  $i$ ,  $\sigma_k^f$  is the microscopic fission cross-section from fissile species  $k$ .

This formulation of the Bateman Equation was first proposed for decay, see Bateman (1910)[26] then expanded for fission and activation as described by Cetnar (2006) [27].

##### Data libraries

To estimate the nuclide composition after build up and decay the code makes use of fundamental nuclear data such as neutronics cross sections (JEF 2.2, Rowlands *et al* (2000) [28]) and decay constants of the considered nuclides. Calculations require input of reactor

neutron flux characteristics, or burnup, power rate and irradiation time. The code provides composition data assessment and their time dependence.

Previously FISPIN has been used by Hiezl *et al* (2015) [29] for the characterization of a UO<sub>2</sub>-spent fuel for disposal studies on spent AGR fuel and for estimating the chemistry and physics of modeling nitride fuels for transmutation, see Thetford & Mignanelli (2003) [21]. It has been used by Mills *et al* (2020) [30] discussing the main issues concerning the fission product build up during burnup but also many interesting issues concerning the behavior and performances of the fuel in pile and as an antineutrino source.

### 3.2 Solid solution formation

#### Formalisation

The relative solubilities in transition metal alloys was found to be due to the sizes of the metal atoms and valence effects by Hume-Rothery (1949) [31]. He proposed rules that describe the conditions under which a metal could dissolve in another metal, forming a solid solution. Atomic radii and volumes fix the miscibility of alloys components, see Hume-Rothery (1966) [32].

The concept of the suited and unsuited sizes in predicting solid solubilities in metallic systems has been revisited. The original concept of Hume-Rothery, involved the use of atomic diameters which were defined as the closest distances of approach of atoms in the crystals of the elements. Atomic diameters correlate better with solid solubilities than do the Goldschmidt atomic diameters and are slightly better than the Pauling single bond metallic radii.

When various crystal structures are involved, the atomic volumes in binary alloys show a rather linear increase with atomic number.

Hume-Rothery's rules were more recently revisited focusing on parameters and phases, Watson & Bennett (2001) [33], on artificial networks, Zhang *et al* (2008) [34] and on the thermodynamics of concentrated solid solution alloys, Gao *et al* (2017) [35]. In order to develop Solid Solution Alloys (SSA), a variety of empirical parameters based on Hume-Rothery rules have been developed.

For solid solutions obtained by substitution, the Hume-Rothery rules are as follows:

1. The crystal structures of solute and solvent have to be similar.
2. The atomic radius ( $r$ ) of the solute (A) and solvent (B) atoms must differ by no more than 15%:

$$\Delta (\%) = (r_A - r_B)/r_B \times 100\% < 15\% \quad (3)$$

3. Complete solubility occurs when the solvent and solute have the same valence. A metal with lower valence is more likely to dissolve in a metal of higher valence.
4. The solute (A) and solvent (B) should have comparable electronegativity ( $\chi$ ):

$$(\chi_{(A)} - \chi_{(B)}) = (eV)^{-1/2} \sqrt{E_d(AB) - (E_d(AA) + E_d(BB))/2} \quad (4)$$

with  $E_d$  the bonding energy (eV). If the electronegativity difference is too great, the metals tend to form intermetallic compounds instead of alloys (solid solutions).

Actually, it is expected that a solid solution that follows the Hume-Rothery rules also follows Vegard's law, see Vegard (1921)[36] :

$$a_{A_xB_{(1-x)}} = x a_A + (1-x) a_B \quad (5)$$

with  $a$  the system lattice parameter (cubic) of  $A_xB_{(1-x)}$  and  $x$  the molar fraction of the solute A. It can be anticipated that the thermodynamic properties of the solid solution are ideal.

In the case of binary nitrides ((M,M')N) a model transposition from the 3 D model of bulk metal alloys (M,M') to the 2D system binary compound solid solutions ((M,M')N) is required. This extrapolation makes sense because nothing concerns explicitly the geometry nor the dimension of the system in the crystallographic approach. This model transposition can be applied to binary nitride solid solutions (see preferential planes (2D) in Fig.2). Subsequently, as it is well known, Vegard's law may be applied to oxide solid solutions e.g. Mieszcynski *et al* (2007)[37] and (M,M')N solid solutions, as compiled for VN, TiN, YN, HfN and ZrN by Johanson *et al* (2018)[38], which may consequently justify the application of Hume-Rothery rules for systems such as salts solid solutions, see Lestari & Lusi (2019)[39] or even nitride solid solutions, see E. Lewin (2020)[40]. It is anticipated that the density of the fuel and its components shall be estimated on the basis of the crystallographic properties of this study.

**Fig 2:** Location of ions in UN fcc structure with ● U ● N.

Note the different planes intercept U and/or N ions according to their orientations. For (100) planes both  $N^{3-}$  and  $U^{3+}$  ions are co-located in the same plane. For the (111) planes the  $N^{3-}$  or  $U^{3+}$  ions are separated over equal distances from one another.

### Data bases

Ionic radii values provided by Shannon and Prewitt (1969)[41] are generally used and are chosen here when specific data are not available. These ionic radii, which were calculated for oxides and fluorides are also appropriate to be used for nitrides with a relatively small error (~5%). For example in nitride and oxide molecules, as reported by Feth (1996) [42], the radii of metal cations are respectively:

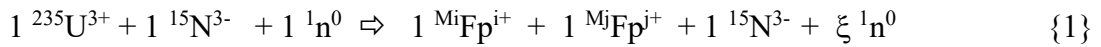
- For  $^{IV}Ru^{3+}$  1.16 Å with nitride and 1.13 Å with oxide ( $\Delta r = 0.03$  Å),
- For  $^{IV}Rb^{1+}$  1.63 Å with nitride and 1.57 Å with oxide ( $\Delta r = 0.06$  Å),
- For  $^{IV}Y^{3+}$  1.28 Å with nitride and 1.22 Å with oxide ( $\Delta r = 0.06$  Å),
- For  $^{IV}Zr^{4+}$  1.21 Å with nitride and 1.15 Å with oxide ( $\Delta r = 0.06$  Å).

Assuming a constant  $N^{3-}$  radius of 1.46 Å, see Baur (1987) [43], the relative difference is  $\leq 5\%$ .

A recent approach based on queries to materials databases followed by evaluation has been reported by Gebhardt & Rappe (2019)[44]. This method could be used to enlarge the set of available ionic radii by proposing radii for missing anionic species and coordination numbers. Electronegativities used here are derived from Pauling (1960)[45]. Data for elements (including actinides) are given by Brown (2012)[46].

#### 4. Spent fuel inventory

The fission reactions in the nitride fuel material can be written as follows:



with  $M_i + M_j + \xi = 235 + 1$  and  $1 \leq \xi \leq 4$ , with  $i \leq 3$  and  $j \leq 3$ , and with  $i + j - 3 = 0$ . The fission reaction takes place with an effective yield of 200% in Fps. A stoichiometric UN at Beginning of Life (BoL) undergoing fission will have a chemistry balanced by its  $\text{N}^{3-}$  ions while the 2 Fps generated at End of Life (EoL), **with a large fraction of  $\text{Fp}^{3+}$  and  $\text{Fp}^0$** , should be balanced by an equivalent number of  $\text{N}^{3-}$  ions. The range of Fps are denoted as follows:

- $\text{M}^{3+}$  (Ln, Y, Zr, Nb),
- $\text{M}^{2+}$  (Ba, Sr),
- $\text{M}^{1+}$  (Cs, Rb),
- $\text{X}^0$  (Xe, Kr),
- $\text{X}^{-1}$  (I, Br).

In addition actinides generated by neutron capture are all  $\text{An}^{3+}$ .

The spent fuel should consequently be formed of a large fraction of soluble nitrides (UN, AnN, LnN, YN, ZrN, NbN) in which grey phases (mixed binary and ternary nitrides) and elementary phases (Mo, Tc, Ru, Rh, Pd) may be found together with (Xe, Kr) precipitates.

**Figure 3** presents the actinide and fission product molar fractions and their charge is mainly balanced by  $\text{N}^{3-}$ . Since all actinides remains  $\text{An}^{3+}$ , the chemical charge balance  $\Delta$  is given by:

$$\Delta = \sum i x_i (\text{Fp}^{i+}) - 3 x (\text{N}^{3-}) \quad (6)$$

with  $x_i$  the molar fraction of the  $\text{Fp}^{i+}$  of valence  $i$  and  $x(\text{N}^{3-})$  the nitride molar fraction. A stoichiometric coefficient  $1 \pm x$  for  $\text{UN}_{1 \pm x}$  may be evaluated, and the physical chemistry of the phases estimated. In these conditions during burn up UN may transition from  $\text{UN}_1$  to  $\text{UN}_{1 \pm x}$ .

The UN inventory was estimated by replacing the  $^{16}\text{O}$  ( $\sigma = 0.00019$  b) with  $^{14}\text{N}$  ( $\sigma = 0.080$  b) and up to 97-99%  $^{15}\text{N}$  ( $\sigma = 0.00004$  b), in the existing oxide-based flux models. The spent fuel composition was calculated at EoL using FISPIN for the following conditions: 4%  $^{235}\text{U}$  (BoL),  $^{15}\text{N}$ , standard LWR. The molar fractions and stoichiometry of fission products and actinides are presented in **Fig. 3** for burnups going from 5 to 60 MW d  $\text{kg}^{-1}$ .

The spent fuel inventories are given for UN fuel after 1 year decay as well as for 5, 30 and 100 years after discharge. The spent fuel composition was obtained from the FISPIN code calculations. The element concentrations refer to Pressurised Water Reactor (PWR) fuel irradiated for 6 years with an irradiation of 60 (high burnup) MW d  $\text{kg}^{-1}$  and 40 MW t $^{-1}$  reactor rating. The differences between the four inventory sets are insignificant for uranium. Compositional changes are due to the other actinides and the fission products during the first hundred years after download. Table 1 gives selected An and Fp concentrations ( $C(t)$ ) for an element M at time  $t$  after discharge and the trend (%) defined as  $100 \times [C(1\text{yr}) - C(100\text{yr})] / C(1\text{yr})$ .

Elements that do not show large changes in concentration (less than 1%) are I, La, Mo, Rh, Xe and Y, while elements that show large variations post irradiation (more than 10%) are Ba, Cs, Pu and Sr; Pm decays totally after 100 years.

**Table 1:** Actinide and fission product concentration in mole per tonne of UN SNF for four times after discharge. Conditions: 60 MW d kg<sup>-1</sup> burnup in PWR, 40 MW t<sup>-1</sup> power rate during 6 years, 4 wt% <sup>235</sup>U enrichment after 1, 5, 30, and 100 years cooling times.

Trend (%) describes the change in element concentration (decay (-) or build-up (+)) at 100 years relative to 1 year after discharge.

Concentration (mol t <sup>-1</sup> )	.after 1 yr	. after 5 yr	. after 30 yr	. after 100 yr	Trend (%)
U	3.89x10 <sup>+3</sup>	3.89x10 <sup>+3</sup>	3.89x10 <sup>+3</sup>	3.89x10 <sup>+3</sup>	0.0
Pu	5.34x10 <sup>+1</sup>	5.21x10 <sup>+1</sup>	4.78x10 <sup>+1</sup>	4.54x10 <sup>+1</sup>	-17.6
La	1.53x10 <sup>+1</sup>	1.53x10 <sup>+1</sup>	1.53x10 <sup>+1</sup>	1.53x10 <sup>+1</sup>	0.0
Ce	3.11x10 <sup>+1</sup>	2.98x10 <sup>+1</sup>	2.98x10 <sup>+1</sup>	2.98x10 <sup>+1</sup>	-4.2
Nd	4.88x10 <sup>+1</sup>	4.97x10 <sup>+1</sup>	4.97x10 <sup>+1</sup>	4.97x10 <sup>+1</sup>	+1.8
Pm	1.01x10 <sup>+0</sup>	3.51x10 <sup>-1</sup>	4.74x10 <sup>-4</sup>	4.40x10 <sup>-12</sup>	-100.0
Y	8.40x10 <sup>+0</sup>	8.40x10 <sup>+0</sup>	8.40x10 <sup>+0</sup>	8.40x10 <sup>+0</sup>	0.0
Zr	6.54x10 <sup>+1</sup>	6.63x10 <sup>+1</sup>	7.01x10 <sup>+1</sup>	7.40x10 <sup>+1</sup>	+13.1
Mo	6.15x10 <sup>+1</sup>	6.15x10 <sup>+1</sup>	6.15x10 <sup>+1</sup>	6.15x10 <sup>+1</sup>	0.0
Rh	6.93x10 <sup>+0</sup>	6.94x10 <sup>+0</sup>	6.94x10 <sup>+0</sup>	6.94x10 <sup>+0</sup>	+0.1
Pd	2.73x10 <sup>+1</sup>	2.85x10 <sup>+1</sup>	2.86x10 <sup>+1</sup>	2.86x10 <sup>+1</sup>	+4.8
Cs	3.60x10 <sup>+1</sup>	3.36x10 <sup>+1</sup>	2.74x10 <sup>+1</sup>	2.11x10 <sup>+1</sup>	-41.4
Ba	2.02x10 <sup>+1</sup>	2.28x10 <sup>+1</sup>	2.94x10 <sup>+1</sup>	3.57x10 <sup>+1</sup>	+76.7
Sr	1.58x10 <sup>+1</sup>	1.49x10 <sup>+1</sup>	1.10x10 <sup>+1</sup>	7.19x10 <sup>+0</sup>	-54.4
Xe	7.03x10 <sup>+1</sup>	7.03x10 <sup>+1</sup>	7.03x10 <sup>+1</sup>	7.03x10 <sup>+1</sup>	0.0
I	3.21x10 <sup>+0</sup>	3.21x10 <sup>+0</sup>	3.21x10 <sup>+0</sup>	3.21x10 <sup>+0</sup>	0.0
Te	6.89x10 <sup>+0</sup>	6.98x10 <sup>+0</sup>	7.03x10 <sup>+0</sup>	7.03x10 <sup>+0</sup>	+2.0
Se	1.14x10 <sup>+0</sup>	1.14x10 <sup>+0</sup>	1.14x10 <sup>+0</sup>	1.14x10 <sup>+0</sup>	0.0

The UN solid solution is the main phase, it comprises in the cationic sub-lattice 87.1 mol% U<sup>3+</sup>, 1.196 mol% Pu<sup>3+</sup>, 0.131 mol% (Np<sup>3+</sup>, Am<sup>3+</sup>, Cm<sup>3+</sup>), 2.662 mol% lanthanides (La<sup>3+</sup>, Ce<sup>3+</sup>, Pr<sup>3+</sup>, ...), 1.660 mol% transition metals (Y<sup>3+</sup>, Zr<sup>3+</sup>, Nb<sup>3+</sup>) for 60 MW d kg<sup>-1</sup> after 1 year following discharge. In addition, for stereochemical reasons, anions such as 0.081 mol% (Br & I) and 0.181 mol% (Se<sup>2-</sup> & Te<sup>2-</sup>) are expected to be found in the anionic N<sup>3-</sup> sub-lattice.

Precipitates as element, noble metal nano-clusters are expected (if the nitrogen potential allows) 3.419 mol% (Mo, Tc, Ru, Rh, Pd), together with the noble gases 1.733 mol% (Kr, Xe).

Alkali metal 0.957 mol% (Rb, Cs) and alkali earth 0.817 mol% (Sr, Ba) will also be present, possibly outside the solid solution. However, because of its large thermal conductivity the fuel is a low temperature fuel, and its central temperature during operation does not reach 800°C. Consequently the formed sub-nano precipitates are expected to remain nanometric in size and not to segregate or recrystallize as micro-phases. At the EoL the UN spent fuel is likely to be slightly hyper-stoichiometric as pointed out by Bradbury & Matzke (1980) [47]. This shall be investigated more in detail in part II of this work.

**Fig 3:** Element concentrations for various decay time after EoL as a function of burnups.

Conditions: Element inventory estimated using FISPIN for UN spent fuel after irradiation in PWR conditions at a power rate 33.58 MW t<sup>-1</sup>, inventory at BoL of the input UN fuel as the initial actinide specifications of 4 wt% <sup>235</sup>U, 3.695x10<sup>-2</sup> wt% of <sup>234</sup>U, 1.5x10<sup>-4</sup> wt% of <sup>236</sup>U and 95.9629 wt% of <sup>238</sup>U and additionally, 99.9 wt% of <sup>15</sup>N and 0.1 wt% of <sup>14</sup>N.



## 5. Crystallographic properties of the solid solution

Emphasis is given to low valence states of actinide and fission product elements because of the reductive conditions of the fuel material prior to irradiation. This section deals with the solid solution phase formed by the nitrides of actinides (An), lanthanides (Ln) and some transition metals (Tr): (U,M)N (M: An, Ln, Tr).

### 5.1 Actinide nitrides in uranium nitride

Uranium mononitride (UN) the spent fuel host matrix of the fuel crystallizes in the fcc system. X-ray absorption fine structure (XAFS) spectroscopy of pure UN has been investigated by Poineau *et al* (2012)[48]. Analysis indicates three uranium shells at distances of 3.46(3), 4.89(5) and 6.01(6) Å. A nitrogen shell is detected at a distance of 2.46(2) Å which corresponds to  $r(\text{U}^{3+}) + r(\text{N}^{3-}) = 2.345$  Å within 5% precision. The lattice parameter of the UN unit cell was determined to be 4.89(5) Å (see Table 2), a result which is in agreement with values obtained by X-ray Diffraction (XRD).

Neptunium and plutonium mononitrides form fcc solid solutions, see Suzuki & Arai, (1998)[49]. The lattice parameter, heat capacity, thermal conductivity and thermal expansion of (U,Pu)N solid solutions were reported by Suzuki *et al* (1991)[50]. This work was completed by the experimental work of Jain & Ganguly (1993)[51] on oxygen properties in UN, PuN and (U,Pu)N.

Akimoto (1967)[52] first investigated the properties of AmN. Tagawa (1971)[53] reported on the phase behaviour and crystal structure of actinide nitrides. The preparation and lattice parameters of actinide mononitrides were also reported by Charvillat (1975)[54]. More recently, thermal expansion and self-irradiation damage in the curium mononitride lattice was published by Takano *et al* (2014)[55]. All these AnN compounds crystallize in the fcc system and their crystallographic data are given in Table 2. They will form solid solutions in the domain given in Fig. 4.

### 5.2 Lanthanide nitrides

The lanthanide nitrides also form fcc structures with lattice constants reducing from 5.30 Å for LaN to 4.76 Å for LuN. There is a clear potential for epitaxial growth e.g. Natali *et al* (2013)[56] which makes their implantation easily supported. In this context the cerium-nitrogen-dopant system was investigated by Brown & Clar (1974)[57]. Accordingly, the rare earth mononitride epitaxial layer includes or consists of at least one rare earth nitride selected from the following group: lanthanum mononitride (LaN), cerium mononitride (CeN), praseodymium mononitride (PrN), neodymium mononitride (NdN), samarium mononitride (SmN), europium mononitride (EuN) and gadolinium mononitride (GdN). Their crystallographic data are given in Table 2. They will also form solid solutions in the domain drawn in Fig. 4.

### 5.3 Transition metal nitrides

Yttrium nitride (YN), zirconium nitride (ZrN) and niobium nitride (NbN) crystallize in the fcc system and also form solid solutions. The crystal structure of YN was described by Kempter *et al* (1957)[58].

Zerr *et al* (2003)[59] proposed a synthesis of cubic zirconium (IV) nitride (Zr<sub>3</sub>N<sub>4</sub>) with the Th<sub>3</sub>P<sub>4</sub> cubic structure, but the compound of interest here is zirconium(III) nitride (ZrN) as described by Harrison & Lee (2016)[60]. Its XAFS analysis revealed three zirconium shells at distances of 3.24, 4.59 and 5.60 Å. A nitrogen shell was also detected at a distance of 2.29 Å, see Olive *et al* (2016)[61], which corresponds to  $r(\text{Zr}^{3+}) + r(\text{N}^{3-}) = 2.29 \text{ \AA}$  using data from Table 2. Niobium nitride was investigated by Brauer & Esselborn (1961)[62] using spectroscopy. The data of these three transition metal nitrides are reported in Table 2. They will form solid solutions in the domain depicted in Fig. 4.

The other (noble) transition metals: molybdenum (Mo), technetium (Tc), ruthenium (Ru), rhodium (Rh) and palladium (Pd) may also form trivalent nitrides.

For molybdenum, the ordered hexagonal phase  $\delta$ -MoN was observed under a nitrogen atmosphere by Machon *et al* (2006)[63]. A fcc MoN compound is also reported; it is however metastable as observed by Linker *et al* (1984)[64].

For technetium, Zhao *et al* (2014)[65] studied stoichiometric technetium nitrides under pressure and found technetium nitrides with various ideal stoichiometries between 0–60 GPa. Tc<sub>3</sub>N and Tc<sub>2</sub>N can be synthesized under ambient conditions and could find application in nuclear waste management. TcN was synthesized by Czerwinski, *et al* (2010)[66].

For ruthenium, Zhang, *et al* (2016)[67] predicted by modelling diverse ruthenium nitrides stabilized under pressure. RuN with a new *I-4m2* symmetry stabilized by pressure was found to be energetically configured instead of fcc as observed by Moreno Armenta *et al* (2007)[68].

For rhodium, RhN data were reported by Du *et al* (2013)[69].

For palladium, the most stable form of PdN crystallizes in zinc-blende structure (fcc). The lattice constants were calculated. Crowhurst *et al* (2008)[70] carried out synthesis and characterization of palladium nitride (isostructural with pyrite) Martinsen & Warlimont (2005)[71]. The data of these three transition metals are reported in Table 2. They are not expected to form solid solutions but are expected to form precipitates in the domain depicted in Fig. 4.

#### 5.4 Application of the Hume-Rothery's rules.

The crystallographic data of actinides, lanthanides and fission product nitrides are given in Table 2 and presented in Fig 4 as a plot of metal electronegativity and M<sup>3+</sup> ionic radius. The solid solution domain emerges from this plot.

Clearly in the solid solution domain Vegard's law, Eq. 3, is applicable as pointed out by Thetford & Mignanelli (2003)[24] which simplifies the situation with regards to the calculation of the fuel density. The UN solid solution includes all AnN (actinide mononitrides) from UN to CmN, all LnN (lanthanide mononitrides) from LaN to GdN and the three first TrN (transition metal mononitrides) YN, ZrN and NbN. Actually, Thetford & Mignanelli (2003)[24] reported that complete solubility would be observed for a relative lattice parameter difference between

-7.5% and +8.5%. The NbN maximum solubility in UN has been estimated to be 50 mol% by Benedict (1977)[72]. Consequently Nb as a fission product should be completely dissolved in the fuel lattice because of its low concentration after irradiation. Note that even if NbN is next to the border of the solubility limit, its concentration in the spent fuel is rather low due to its low production yield during fission see Fig. 3. Concerning the density, AmN and CmN data are affected by radiation swelling. Lanthanide redox issues may affect some of the data e.g. Eu(II) nitride. For the transition metals mononitrides, some are reported metastable, not crystallising in fcc or present with allotropic varieties of subnitrides. TcN, RuN and PdN are not reported in standard conditions in Table 2.

**Fig. 4.** Actinides, lanthanides and transition metals nitrides are displayed in a - electronegativity ( $\chi$ ) versus  $M^{3+}$  ionic radius ( $r$ ) scheme. The nitride **Solid Solution** and **Precipitate** domains are highlighted, data from Table 2, NbN is partially soluble however in the spent fuel its concentration is small (see Fig. 3).

**Table 2.**  $M^{3+}$  nitrides (MN) crystallographic data. Conditions: all MN systems are fcc with  $\alpha=\beta=\gamma=90^\circ$ ,  $N^{3-}$  ionic radius: 1.32(4) Å,  $\chi(N)$ : 3.04. **MN** in **Bold** at least 50% miscible in UN, natural molecular weight except (), \* estimated,  $P \neq 1$  not in standard conditions.

MN	$M$ (g mol <sup>-1</sup> )	System	$a=b=c$ (Å)	$r(M^{3+})$ (Å)	$100\Delta r/r$ (%)	$\rho$ (g cm <sup>-3</sup> )	$\chi$ (-)	Reference
<b>UN</b>	252	.fcc	4.8889	1.025	-	14.32	1.38	Suzuki <i>et al</i> (1991) [50]
<b>NpN</b>	(251)	.fcc	4.897	1.01	-1.5	14.20	1.36	Suzuki <i>et al</i> (1991) [50]
<b>PuN</b>	(254)	.fcc	4.905	1.00	-2.4	14.40	1.28	Suzuki <i>et al</i> (1991) [50]
<b>AmN</b>	(256)	.fcc	4.991	0.975	-4.9	-	1.13	Akimoto (1967) [52]
<b>CmN</b>	(258)	.fcc	5.026	0.97	-5.4	-	1.28	Takano <i>et al</i> (2014) [55]
<b>LaN</b>	152.91	.fcc	5.305	1.032	+0.7	9.3*	1.10	Natali <i>et al</i> (2013) [56]
<b>CeN</b>	154.12	.fcc	5.020	1.01	-1.5	7.89	1.12	Brown <i>et al</i> (1974) [57]
<b>PrN</b>	154.91	.fcc	5.135	0.99	-3.4	7.46	1.13	Natali <i>et al</i> (2013) [56]
<b>NdN</b>	158.25	.fcc	5.132	0.983	-4.1	7.70	1.14	Natali <i>et al</i> (2013) [56]
<b>PmN</b>	(159)	.fcc	5.08*	0.97	-5.4	7.5*	1.13	Natali <i>et al</i> (2013) [56]*
<b>SmN</b>	165.92	.fcc	5.035	0.958	-6.5	7.35	1.17	Natali <i>et al</i> (2013) [56]
<b>EuN</b>	165.97	.fcc	5.017	0.947	-7.6	8.7*	1.20	Natali <i>et al</i> (2013) [56]
<b>GdN</b>	171.26	.fcc	4.974	0.938	-8.5	7.6*	1.20	Natali <i>et al</i> (2013) [56]
<b>YN</b>	102.913	.fcc	4.877	1.04	+1.5	5.60	1.22	Kempton <i>et al</i> (1957) [58]
<b>ZrN</b>	105.23	.fcc	4.575	0.97	-5.4	7.09	1.33	Harrison <i>et al</i> (2016) [60]
<b>NbN</b>	106.91	.fcc	4.442	0.86	-16.1	8.47	1.60	Brauer <i>et al</i> (1961) [62]
<b>MoN</b>	109.95	.fcc	4.212	0.83	-19.0	9.20	2.16	Linker <i>et al</i> (1984) [64]
<b>TcN</b>	111.91	fcc	3.980	0.83	-19.0	$P \neq 1$	1.90	Zhao <i>et al</i> (2014) [65], Song <i>et al</i> (2016) [73] $\leq$
<b>RuN</b>	115.08	.fcc	4.445	0.82	-20.0	$P \neq 1$	2.20	Moreno <i>et al</i> (2007) [68]
<b>RhN</b>	116.91	.fcc	3.271	0.805	-21.5	7.85	2.28	Du <i>et al</i> (2013) [69]
<b>PdN</b>	120.42	.fcc	3.8902	0.78	-23.9	11.98	2.20	Martinsen <i>et al</i> (2005)[71]

## 6 Crystallographic properties of the precipitates

### 6.1 Grey phases $MN_n$ and $MX_x$

Grey phases are found with alkaline earths, alkali metals nitrides and halides  $MN_n$  and  $MX_x$  as well as  $UX_x$  in UN. They do not form solid solutions but should precipitate in the domain depicted in Fig. 5.

#### Binary nitrides

Light alkali metal binary nitrides (e.g.  $\text{Li}_3\text{N}$  and  $\text{Na}_3\text{N}$ ) have been identified by Gregory (2001)[74]. However, both cesium nitride ( $\text{Cs}_3\text{N}$ ) and rubidium nitride ( $\text{Rb}_3\text{N}$ ) are unstable. They were not found by synthesis and modelling predicts their instability. At ambient pressure nitrides such as  $\text{Cs}_2\text{N}$  and  $\text{Cs}_5\text{N}$  are postulated, and, at high pressure, exotic cesium polynitrides may be expected, Peng *et al* (2015)[75].

Nitrides may be formed with earth alkaline metals. Barium nitride ( $\text{Ba}_3\text{N}_2$ ) crystallises in a cubic system. Ehrlich (1963)[76] investigated strontium nitride ( $\text{Sr}_3\text{N}_2$ ) and barium nitride ( $\text{Ba}_3\text{N}_2$ ). Strontium nitride (fcc) because of its smaller ionic radius could partially be soluble in UN. Barium nitride, however, cannot form solid solutions with UN at high concentration because the ionic radius of  $\text{Ba}^{2+}$  is too large and because of their difference in electronegativity.

### Binary halides

In UN, because of the reducing conditions of the fuel, I and Br must be present as iodide and bromide. They could form  $\text{UBr}_3$  and  $\text{UI}_3$  respectively, see Levy *et al* (1975) [77].

$\text{UI}_3$  has a melting point of  $766^\circ\text{C}$ . It is orthorhombic with lattice constants  $a = 4.334$ ,  $b = 14.024$ ,  $c = 10.013 \text{ \AA}$  ( $Z=4$ ), see Murasik *et al* (1981)[78].  $\text{UI}_3$  will consequently precipitate in UN. Both halides could also be found as CsI or CsBr which would also be expected to precipitate in UN.

### Binary chalcogenides

Selenides and tellurides of uranium have been produced by solid-vapour reaction and densified by melting, see Matson *et al* (1963) [79]. Melting points were estimated and some structures were determined by X-ray analysis.  $\text{USe}$  and  $\text{UTe}$  were both found to be fcc, as reported by Kruger & Moser (1967) [80]. These two chalcogenides are those likely to be found in the spent fuel, however, here U is bivalent. Data on trivalent uranium chalcogenides:  $\text{U}_2\text{Se}_3$  and  $\text{U}_2\text{Te}_3$  are reported by Grenthe *et al* (2006) [81]. Suski *et al* (1976) [82] investigated these uranium sesquichalcogenides for their magnetic properties. Tougait *et al* (2001) [83] produced two binary uranium tellurides  $\text{U}_3\text{Te}_5$  and  $\text{U}_2\text{Te}_3$  for neutron diffraction studies. Salamat *et al* (2014) [84] synthesized  $\text{U}_3\text{Se}_5$  and  $\text{U}_3\text{Te}_5$  by combining high pressure-temperature and chemical precursor approach.

$\text{Cs}_2\text{Te}$  and  $\text{Cs}_2\text{Se}$  as well as  $\text{Rb}_2\text{Te}$  and  $\text{Rb}_2\text{Se}$  should have the  $\text{K}_2\text{S}$  structure (antifluoride) in the spent fuel. Böttcher (1980) [85] reported that  $\text{Rb}_2\text{Te}_3$  crystallizes with a *Pnma* (space group) structure whereas  $\text{Cs}_2\text{Te}_3$  has an orthorhombic structure. Both structures contain  $\text{Te}_3^{2-}$  polyanions, features which would be unlikely to be found in the spent fuel.

The data of the heavy alkaline earths, alkali metals nitrides, halides and chalcogenides are reported in Table 3.

### Ternary chalcogenides

Several  $\text{M}_m\text{U}_u\text{Q}_q$  compounds have been synthesised and characterised. Ternary selenides such as  $\text{K}_4\text{USE}_8$  prepared by Sutorik *et al* (1991) [86] crystallize in the orthorhombic system.

A similar telluride compound  $\text{CsUTE}_6$  has been synthesized by Cody *et al* (1995) [87], Cody & Ibers (1995)[88]. This materials comprise  $\text{Cs}^+$  cations and one-dimensional chain anions.  $\text{CsUTE}_6$  crystallizes also in the orthorhombic system with eight formula units including chain structures in a cell of dimensions  $a = 30.801(7)$ ,  $b = 8.143(2)$ ,  $c = 9.174(2) \text{ \AA}$ .

More complex  $\text{M}_m\text{U}_u\text{Q}_q$  compounds are also known such as  $\text{Cs}_3\text{U}_{18}\text{Se}_{38}$  which was prepared and characterised by the same group (Oh & Ibers, 2012) [89].

## Ternary nitrides

Numerous ternary nitrides may be formed with strontium and barium. Gregory *et al* (1996) [90] synthesised and characterised a new layered ternary nitride, SrZrN<sub>2</sub>. Diffraction data for SrZrN<sub>2</sub> revealed the hexagonal nature of this material (a: 3.373 Å and c: 17.676 Å). Other compounds such as CsZrN<sub>2</sub>, RbZrN<sub>2</sub>, CsMoN and RbMoN need to be considered.

## Ternary nitride halides

Bowman *et al* (2006) [91] synthesized and characterized nitrides including iodide and bromide in the form of ternary and quaternary strontium nitride halides: Sr<sub>2</sub>N(Br,I). Bailey *et al* (2007)[92] revisited the crystal growth and characterization of strontium nitride iodide, Sr<sub>2</sub>NI. The only well-characterized lanthanide nitride iodide Ce<sub>15</sub>N<sub>7</sub>I<sub>24</sub>, was synthesised by Mattausch *et al* (2010) [93] following the reaction of CeI<sub>3</sub> and CeN (8:7 mole) at 1050 K in sealed tubes.

## Ternary nitride chalcogenides

Lanthanide nitride chalcogenides (Ln<sub>1</sub>N<sub>n</sub>Q<sub>q</sub>, with Q= Se or Te) have been extensively studied over the last 40 years. The most relevant compounds are:

- M<sub>3</sub>NQ<sub>3</sub>: Ce<sub>3</sub>NSe<sub>3</sub> was characterised by Lissner & Schleid (2004) [94], Dy<sub>3</sub>NSe<sub>3</sub> and Ho<sub>3</sub>NSe<sub>3</sub> was studied by Lissner & Schleid (2009) [95] and the phase Gd<sub>3</sub>NSe<sub>3</sub> which crystallizes in the orthorhombic system was studied by Schurz *et al* (2013) [96],
- M<sub>4</sub>N<sub>2</sub>Se<sub>3</sub> with Nd<sub>4</sub>N<sub>2</sub>Se<sub>3</sub> and Tb<sub>4</sub>N<sub>2</sub>Se<sub>3</sub> studied by Lissner & Schleid (2003) [97], Pr<sub>4</sub>N<sub>2</sub>Se<sub>3</sub> characterised by Lissner & Schleid (2005) [98], Ce<sub>4</sub>N<sub>2</sub>Se<sub>3</sub> and Ce<sub>4</sub>N<sub>2</sub>Te<sub>3</sub> investigated by Schurz & Schleid (2012) [99] and the series M<sub>4</sub>N<sub>2</sub>Te<sub>3</sub> for La-Nd described by Lissner & Schleid (2005) [100] as first nitride tellurides of the lanthanide group,
- M<sub>5</sub>NSe<sub>6</sub> with Pr<sub>5</sub>NSe<sub>6</sub> were characterised by Lissner *et al* (2005)[101] and the series of M<sub>5</sub>NSe<sub>6</sub> for M= La-Pr studied by Schurz *et al* (2011) [102].

In these compounds the lanthanide metals have a trivalent oxidation state, however their relatively complex structures make them difficult to form in the UN spent fuel. By contrast Ce<sub>2</sub>SeN<sub>2</sub> characterised by Dong & DiSalvo (2011)[103] displays a more simple stoichiometry that could form in the spent fuel. However, this selenide nitride contains tetravalent cerium which is unlikely in this non-oxidising fuel.

All of the above compounds of fission products including metal halides, chalcogenides and nitrides could be produced, however their relatively complex structures and their restricted concentration make them difficult to form in the UN spent fuel. A more complete approach including thermodynamic estimation is needed (see part II of this paper).

**Fig. 5.** Uranium (U<sup>3+</sup>), alkaline earth (M<sup>2+</sup>) and alkali (M<sup>1+</sup>) metals nitrides and halides (X<sup>1-</sup>) displayed in an electronegativity ( $\chi$ ) versus ionic radius ( $r$ ) scheme. **Solid Solution** and **Precipitate** domains are highlighted, **Sr<sup>2+</sup>** (Sr<sub>3</sub>N<sub>2</sub>) and **Ba<sup>2+</sup>** (Ba<sub>3</sub>N<sub>2</sub>) are lying between both domains suggesting partial solubility, **Rb<sub>3</sub>N** and **Cs<sub>3</sub>N** are hypothetically estimated.

**Table 3.**  $U^{3+}$ ,  $M^{2+}$  and  $M^{1+}$  nitrides, chalcogenides and halides crystallographic data.  $N^{3-}$  ionic radius: 1.32(4) Å,  $\chi(N)$ : 3.04, P under pressure > 1 GPa. Data for  $Cs_3N$  and  $Rb_3N$  are hypothetically estimated. Binary compounds only; the data shows that these phases do not co-crystallise in the UN fcc phase; for references see text.

$M_mN_n$	$M$ (g mol <sup>-1</sup> )	System	a,b,c (Å)	$\alpha,\beta,\gamma$ (°)	$r(M^{i+})$ (Å)	100 $\Delta r/r$ (%)	$\rho$ (g cm <sup>-3</sup> )	$\chi$ (-)
UN	(252)	.fcc	4.8889	90	1.025	-	14.32	1.38
$Ba_3N_2$	439.99	.fcc	5.369	90	1.49	+45.4	4.72	0.89
$Sr_3N_2$	290.87	.fcc			1.32	+28.8	4.10	0.95
$Cs_3N$	412.72	Not found	-	-	1.81	+76.6	-	0.79
$Rb_3N$	270.41	Not found	-	-	1.66	+62.0	-	0.82
CsI	259.81	.fcc	5.557	90	2.06	+47 Vs $N^{3-}$	3.55	2.66
CsBr	212.81	.fcc	4.393	90	1.82	+30 Vs $N^{3-}$	4.17	2.96
$Cs_2Te$	393.4	Ortho- rhom- bic	5.917 9.527 11.62	90	2.07	+48 Vs $N^{3-}$	3.99	2.10 Te
$Cs_2Se$	344.8	Ortho- rhom- bic	4.986 6.488 9.228	90	1.84	+31 Vs $N^{3-}$	3.84	2.55 Se
$UI_3$	618.74	Ortho- rhom- bic	4.354 14.024 10.013	90	1.025 U 2.06 I	- +47 Vs $N^{3-}$	6.78	1.38 U 2.66 I
$UBr_3$	477.74	Hexa- gonal	7.942 7.942 4.441	90 90 120	1.025 U 1.82 Br	- +30 Vs $N^{3-}$	6.42	1.38 U 2.96 Br
$\beta$ - $U_2Te_3$	858.86	Ortho- rhom- bic	12.175 4.370 11.828	90	1.025 U 2.07 Te	- +48 Vs $N^{3-}$	9.06	1.38 U 2.10 Te
$U_2Se_3$	858.86	Ortho- rhom- bic	10.940 11.330 4.060	90	1.025 U 1.84 Se	- +31 Vs $N^{3-}$	9.40	1.38 U 2.55 Se

## 6.2 Precipitates with element fission products UN – M , UN - X

**Molybdenum** (Mo) may form low valence state nitrides. A subnitride such as  $\gamma$ -Mo<sub>2</sub>N (Fm-3m, fcc,  $a = 4.18 \text{ \AA}$ ) was found stable up to 54 GPa and 2000 K under argon atmosphere. Additional reflections of the hexagonal phase  $\delta$ -MoN (P63mc,  $a = 5.733 \text{ \AA}$  and  $c = 5.608 \text{ \AA}$ ) were also recorded under these conditions but under nitrogen. Molybdenum metal crystallises in the bcc system, its properties have recently been described by Mitchell *et al* (2020)[104]. Ternary transition metal nitrides such as NbMoN produced by ammonolysis crystallise in the Fm-3m fcc cubic type as reported by Himri *et al* (2015) [105].

For **technetium** (Tc), the existence of hexagonal Tc<sub>3</sub>N and Tc<sub>2</sub>N sub-nitrides have been synthesized from the elements and investigated. These Tc subnitride phases were compared with bulk Tc and Tc mononitride in order to draw relationships between the structures for the different Tc/N stoichiometries. Information on technetium metal may be found in the work of Cordero *et al* (2008)[106]. It is found to be hcp. Here, in the spent nitride fuel, Tc may be expected to be metallic as observed by Hania *et al* (2015)[19].

The behaviour of **ruthenium**, **rhodium** and **palladium** in UN may be described as follows. Ab initio calculations were performed by Rajeswarapalanichamy *et al* (2014) [107] to investigate the structural stability of 4d transition metal nitrides TrN (Tr = Ru, Rh, Pd) for five crystal structures, namely NaCl, CsCl, ZnS, NiAs and (Fe,Zn)S (wurtzite). Among these crystal structures, the zinc-blende structure was found to be the most stable among all three nitrides at normal pressure. RuN however decomposes above 100°C, see Moreno-Armeta *et al* (2007).

A mononitride such as PdN which crystallizes in the fcc structure under pressure was found to be the most stable nitride. Crowhurst *et al* (2008)[57] synthesised and characterized this palladium nitride.

In the UN reducing conditions, ruthenium, rhodium and palladium are expected to be in metallic form. Their properties may be found in Renner *et al* (2002)[108]. However, these transition metals may also react with UN. The early work by Fee & Johnson (1975)[109] suggests the possible formation of U(Pd,Rh,Ru)<sub>3</sub>. Uno *et al* (1997) [110] investigated **reactions** of uranium nitride with platinum-family metals. Their reaction with uranium nitrides at temperatures ranging from 873 to 1673 K under nitrogen from  $\sim 10^{-2}$  to  $\sim 10^5$  Pa was analysed by XRD and SEM/EDX. The reactions between UN and Ru or Rh with 0.33 molar ratio yielded the intermetallic compounds URu<sub>3</sub> or URh<sub>3</sub> respectively. UPd<sub>4</sub> phase was formed in addition to UPd<sub>3</sub> in the reaction between UN and Pd. These metals form compounds with uranium quite easily and will precipitate as intermetallics because their structures are not fcc and their radii are larger than U<sup>3+</sup>.

Properties of uranium intermetallic compounds UPd<sub>3</sub>, URh<sub>3</sub>, URu<sub>3</sub> were investigated by Yamanakaa *et al* (1998) [111]. These intermetallic compounds are all cubic with lattice parameter values (a) 5.774, 3.975 and 3.993 Å respectively.

Nitride - metal mixed phases such as Mo<sub>2</sub>N-Pd have also been investigated. Yan *et al* (2018) [112] investigated the synergism of molybdenum nitride and palladium. It was shown that well dispersed small grain Mo<sub>2</sub>N is favorable for Pd deposition **to form strongly associated Mo<sub>2</sub>N-Pd structures**.



The noble gases, **xenon** (Xe) and **krypton** (Kr), form generally in spent fuel separate nanophases that are erroneously called bubbles referring to their gaseous nature. It was observed that in spent MOX these nanophases are solid precipitates (and not bubbles) as reported by Degueldre *et al* (2014)[113]. It may be anticipated that this is also the case in UN spent fuel. Solid krypton at the temperature of liquid hydrogen boiling under normal pressure, exhibit Debye-Scherrer diffraction features when radiated with unfiltered iron or filtered copper X-rays, Keesom & Mooy (1930)[114]. The lattice constant is 5.59 Å. The calculated density is 3.13 g cm<sup>-3</sup>. The distance of the centres of neighbouring krypton atoms amounts to 3.96 Å, whereas from viscosity measurements the value 3.23 Å is deduced for the diameter of the atoms. The analogous ratio for xenon is 1.23. Xenon data are found in Sears & Klug (1962)[115]. A lattice parameter value of 6.1317±0.0005 Å is obtained extrapolated to 0 K.

The data of the noble transition metals and noble gases are reported in Table 4. They do not form solid solutions but precipitates in the domain depicted in Fig. 6.

**Fig. 6.** Uranium, noble transition metals and noble gases displayed in a - electronegativity ( $\chi$ ) versus atom radius ( $r$ ) scheme. **Solid Solution** and **Precipitates** domains are highlighted.

**Table 4.** Noble transition metals and noble gases crystallographic data.  $N^{3-}$  ionic radius: 1.32(4) Å,  $\chi(N)$ : 3.04;  $N$  refers to the number (coordination) of neighbour atoms. For references see text. The data show that these phases do not co-crystallise in the UN fcc phase.

MN	$M$ (g mol <sup>-1</sup> )	System	a,b,c (Å)	$\alpha,\beta,\gamma$ (°)	$r$ (M <sup>3+</sup> ) (Å)	$\rho$ (g cm <sup>-3</sup> )	$\chi$ (-)
UN	252.0	fcc	4.8889	90	1.025	14.32	1.38
					$r$ (M <sup>0</sup> ) (Å)		
Mo	95.95	bcc	3.1470	90	1.45	10.28	2.16
Tc	99	hcp	2.735-4.388	90, 60	1.35	11.50	1.90
Ru	101.07	hcp	2.706-4.282	90, 60	1.30	12.37	2.20
Rh	102.91	fcc	3.8034	90	1.35	12.41	2.28
Pd	106.42	fcc	3.8907	90	1.40	12.02	2.20
					$r$ (X <sup>0</sup> ) (Å)		
URu <sub>3</sub>	541.24	Pm3m	3.993	90	1.30	14.03	1.38 U 2.20 Ru
URh <sub>3</sub>	546.80	Pm3m	3.975	90	1.35	13.86	1.38 U 2.28 Rh
UPd <sub>3</sub>	557.29	Pm3m	5.774	90	1.40	12.89	1.38 U 2.20 Pd
					$r$ (X <sup>0</sup> ) (Å)		
Kr	83.80	.fcc	5.706	90	1.78 ( $N$ : 6)	~2.8	3.00
Xe	131.29	.fcc	6.2023	90	1.96 ( $N$ : 6)	3.64	2.80

## 7 Discussion

In contrast with UOx, UN spent fuel is expected, as seen for example in Fig.1, to form a rather continuous and homogeneous material which is locally decorated by microscopic pores and nanoscopic precipitates.

The **density** of uranium nitride fuel is an important parameter to be **investigated** in order to guarantee the fuel performance. It is necessary to have an understanding of the type of density being measured as well as the type of material in question.

For the homogeneous fuel, the density is its total mass divided by its total volume. The fuel density has however to be first corrected by the porosity. The corrected bulk density is then that of the solid solution corrected for the precipitated phases by their component fractions. For the precipitates then their density varies between different regions of the fuel specimen according to their nature, see Table 3 for insoluble nitrides, chalcogenides and halides, and, Table 4 for metals and intermetallic alloys as well as noble gases precipitates.

Partial reduction of uranium nitride in heminitride during burnup is unlikely. Zhou *et al* (2018) [116] explored the possible stable stoichiometries of the U-N systems with  $U_mN_n$  compositions from 0 to 150 GPa using a swarm intelligence-based structural prediction based on the first-principles calculations. They found  $U_2N$  at 50 GPa with the Cmca structure and  $U_2N$  at 100 GPa with the C2/m structure. For U-rich compounds,  $U_2N$  becomes a stable stoichiometry of U-N system above 50 GPa, and it first adopts an **orthorhombic** structure and then undergoes a pressure-induced phase transition to a **monoclinic** phase at 98.0 GPa. Especially, it is noticed that  $U_2N$  undergoes a pressure-induced phase transition with a large volume collapse of 38.7%.

Here these pressures that are not expected in this advanced fuel could exist in the vicinity of (Xe,Kr) nano-phases also wrongly called bubbles, see Degueldre *et al* (2014) [114].

Resulting from the **Hume-Rothery's** rules the elements that belong to the solid solution (An,Ln,Tr)N have of course a 1/1 stoichiometry with nitrogen, as depicted in Fig. 3. In this Figure all the other elements form precipitates that can be alkaline or alkaline earth metals i.e. Cs, Rb and Ba, Sr halides (I, Br) and /or chalcogenides (Te, Se). These later can also combine with uranium (III).

Here the **Hume-Rothery's** rules have helped to understand in which form an element is expected to be found.

For the transition metal it is clear from Fig 5 that Y, Zr and Nb will form YN, ZrN and NbN, which are found in the solid solution with UN. The situation may be somewhat ambiguous for Mo and Tc for which some nitride could be found (minor fraction only). Ru, Rh and Pd are expected definitively as metal and more specifically as intermetallic as outlined in Section 6.2 (see data in Table 4). Density is also a function of porosity, defects and consequent swelling due to irradiation

Because of the low temperature of the fuel, the Fps are expected to be soluble or nano-dispersed precipitates. Microscopic precipitated phases are not expected when the spent fuel has not undergone high temperature excursions during its lifetime. The density of the fuel and its components can be estimated on the basis of the crystallographic properties reported in this study. The speciation has to be consequently confirmed by investigating the spent fuel using a thermodynamic approach. The approach could be completed by computational means such as density functional theory for determining phase stability. This may however be difficult because many potentials of the Fps are unknown in such a complex nitride matrix.

## 8 Conclusion

Uranium nitride fuel is being considered because of its higher fissionable density, acceptable swelling, higher thermal conductivity, lower operating temperatures and high melting temperature compared to the most common nuclear fuel, UO<sub>2</sub>. It demonstrates consequently lower fission gas release. It also shows little chemical reactivity with cladding materials.

During burn up the fission reaction yield is 200%, however when UN fissions it releases less nitride ions than the produced Fps. A majority of Fps are M<sup>3+</sup> (Ln, Y, Zr, Nb) recrystallising in fcc solid solution with UN and the other actinides formed during burnup. The stability of the solid solution is dictated by the Hume-Rothery rules. The other Fps are M<sup>2+</sup> (Ba, Sr) and M<sup>1+</sup> (Cs, Rb) while some elements are M<sup>0</sup> (Mo, Tc, Ru, Rh, Pd) as well as X<sup>0</sup> (Xe, Kr), X<sup>-1</sup> (I, Br) and X<sup>-2</sup> (Te, Se). These fission products may form nano-precipitates. Actinides gained by neutron capture on <sup>238</sup>U are all An<sup>3+</sup> which are also found in fcc solid solution.

The spent fuel is consequently formed of a large fraction of soluble nitrides (U, An's, Ln's, Y, Zr, Nb)N forming a solid solution according to Hume-Rothery rules. This phase follows also Vegard's law. The UN spent fuel material is expected to be rather homogeneous as found in the CONFIRM PIE of the (Zr, Pu)N spent fuel material as well as found by ab-initio modelling of Ln, Y, Zr, Nb, incorporated in UN. Because of the low temperature of the fuel, the FPs are expected to be soluble or nano-dispersed precipitates. Microscopic precipitated phases are not expected when the spent fuel has not undergone high temperature trip excursions during its lifetime. The density of the fuel and its components can be estimated on the basis of the crystallographic properties reported in this study. A second

paper will study the thermodynamic properties of the fuel and its components to justify the build-up of the phases during burnup and after discharge.

## Acknowledgements

This research was funded under the £46m Advanced Fuel Cycle Programme as part of the Department for Business, Energy, and Industrial Strategy's (BEIS) £505m Energy Innovation Programme.

## Credit

All author/co-author participated actively to the production of the paper.

C. Degueldre, reviewed and revisited literature and crystallographic data, performing specific calculations

D. Goddard, carried out the calculations of the stoichiometry of the spent fuel and the editing, management at>NNL

G. Berhane, contributed to the assessment of the data via experimental work and to specific calculations using FISPIN,

A. Simpson, performed FISPIN calculations

C. Boxall, editing, management at LU.

## References

---

- [1] A.A. Bauer, *Nitride fuels: properties and potentials*, Reactor Technology, 15 (1972) 87-104.
- [2] C. Ekberg, D. Ribeiro Costa, M. Hedberg, M. Jolkkonen, *Nitride fuel for Gen IV nuclear power systems*, J. Radioanal. Nucl. Chem., 318 (2018) 1713-1725. <https://doi.org/10.1007/s10967-018-6316-0>
- [3] N.R. Brown, A. Aronson, M. Todosow, R. Brito, K. J. McClellan, *Neutronic performance of uranium nitride composite fuels in a PWR*, Nuclear Engineering and Design 275 (2014) 393–407. <http://dx.doi.org/10.1016/j.nucengdes.2014.04.040>
- [4] R. B. Matthews, K. M. Chidester, C. W. Hoth, R. E. Mason, R. L. Petty, *Fabrication and testing of uranium nitride fuel for space power*. J. Nucl. Mater., 151 (1988) 345. [https://doi.org/10.1016/0022-3115\(88\)90029-3](https://doi.org/10.1016/0022-3115(88)90029-3)
- [5] C.G.W. Silva, C.B. Yeamans, A.P. Sattelberger, T. Hartmann, G.S. Cerefice, K.R. Czerwinski. *Reaction Sequence and Kinetics of Uranium Nitride Decomposition*. Inorg. Chem., 48 (2009) 10635-10642. <https://doi.org/10.1016/j.jnucmat.2018.02.041>
- [6] V. J. Tennery, T. G. Godfrey, R. A. Potter, *Sintering of UN as a Function of Temperature and N<sub>2</sub> Pressure*, J. Am. Ceram. Soc, 54 (1971) 327-331. <https://doi.org/10.1111/j.1151-2916.1971.tb12306.x>
- [7] U. Carvajal Nunez, D. Prieur, R. Bohler, D. Manara, *Melting point determination of uranium nitride and uranium plutonium nitride: A laser heating study*, J. Nucl. Mater., 449 (2014) 1-8. <https://doi.org/10.1016/j.jnucmat.2014.02.021>

--

- 
- [8] A. V. Lunev, V. V. Mikhalechik, A. V. Tenishev, V. G. Baranov, *Kinetic and microstructural studies of thermal decomposition in uranium mononitride compacts subjected to heating in high-purity helium*, J. Nucl. Mater., 475 (2016) 266-273. <https://doi.org/10.1016/j.jnucmat.2016.04.018>
- [9] H. Inouye, J. M. Leitnaker, *Equilibrium Nitrogen Pressures and Thermodynamic Properties of UN* J. Am. Ceram. Soc, 51 (1968) 6-9. <https://doi.org/10.1111/j.1151-2916.1968.tb11818.x>
- [10] S.L.Hayes, J.K.Thomas, K.L.Peddicord, *Material property correlations for uranium mononitride: I. Physical properties*, J. Nucl. Mater., 171 (1990) 262-270. [https://doi.org/10.1016/0022-3115\(90\)90374-V](https://doi.org/10.1016/0022-3115(90)90374-V)
- [11] G. Kim, S. Ahn, *Thermal conductivity of gadolinium added uranium mononitride fuel pellets sintered by spark plasma sintering*, J. Nucl. Mater., 546 (2021) 152785. <https://doi.org/10.1016/j.jnucmat.2021.152785>
- [12] Y.Takahashi, M.Murabayashi, Y.Akimoto, T.Mukaibo, *Uranium mononitride: Heat capacity and thermal conductivity from 298 to 1000 K*. J. Nucl. Mater. 38 (1971) 303-308 [https://doi.org/10.1016/0022-3115\(71\)90059-6](https://doi.org/10.1016/0022-3115(71)90059-6)
- [13] R.L. Martin, J.E. Gates, D.L. Keller, V.W. Storhok, W.J. Zielenbach, U.S. Atomic Energy Commission., Joint U.S.-Euratom Research and Development Program., Battelle Memorial Institute. (1965). *Radiation stability of uranium mononitride*. Columbus, Ohio: Battelle Memorial Institute. <https://babel.hathitrust.org/cgi/pt?id=mdp.39015095025576&view=1up&seq=3>
- [14] K. D. Johnson, D. Adorno Lopes, *Grain growth in uranium nitride prepared by spark plasma sintering*, J. Nucl. Mater., 503 (2018) 75-80. <https://doi.org/10.1016/j.jnucmat.2018.02.041>
- [15] V. G. Baranov, A. V. Tenishev, R. S. Kuzmin, S. A. Pokrovskiy, E. S. Solntseva, *Thermal stability investigation technique for uranium nitride*, Ann. Nucl. Energy, 87 (2016) 784-792. <https://doi.org/10.1016/j.anucene.2014.09.023>
- [16] C. Degueldre, T. Yamashita, *Inert matrix fuel strategies in the nuclear fuel cycle: the status of the initiative efforts at the 8th Inert Matrix Fuel Workshop*, J. Nucl. Mater., 319 (2003) 1-5. [https://doi.org/10.1016/S0022-3115\(03\)00126-0](https://doi.org/10.1016/S0022-3115(03)00126-0)
- [17] M. Streit, *Fabrication and Characterisation of (Pu,Zr)N Fuels*. Thesis for: PhD (2004) ETHZ. <https://doi.org/10.3929/ethz-a-004674329>
- [18] M. Klipfel, V. Di Marcello, A. Schubert, J. van de Laar, P. Van Uffelen, *Towards a multiscale approach for assessing fission product behaviour in UN*, J. Nucl. Mater., 442 (2013) 253-261. <https://doi.org/10.1016/j.jnucmat.2013.08.056>
- [19] P. R. Hania, F. C. Klaassen, B. Wernli, M. Streit, R. Restani, F. Ingold, A.V. Fedorov, J. Wallenius, *Irradiation and post-irradiation examination of uranium-free nitride fuel*, J. Nucl. Mater., 466 (2015) 597-605. <https://doi.org/10.1016/j.jnucmat.2015.08.054>
- [20] Y. Arai, A. Maeda, Ken-ichi Shiozawa, T. Ohmichi, *Chemical forms of solid fission products in the irradiated uranium—plutonium mixed nitride fuel*, J. Nucl. Mater. 210 (1994) 161 -166. [https://doi.org/10.1016/0022-3115\(94\)90233-X](https://doi.org/10.1016/0022-3115(94)90233-X)
- [21] R. Thetford, M. Mignanelli *The chemistry and physics of modelling nitride fuels for transmutation*, J. Nucl. Mater. , 320 (2003) 44 – 53. [https://doi.org/10.1016/S0022-3115\(03\)00170-3](https://doi.org/10.1016/S0022-3115(03)00170-3)
- [22] R. Burstall, *FISPIN- a computer code for nuclide inventory calculations (ND-R—328 (R))*. U K. 1979.

- 
- [23] FISPIN10A – Spent nuclear fuel inventory code suite. Developed by the UK National Nuclear Laboratory and distributed by the ANSWERS software service; Available from: [www.answerssoftwareservice.com](http://www.answerssoftwareservice.com).
- [24] T. Newton, G. Hosking, L. Hutton, D. Powney, B. Turland and E. Shuttleworth, *Developments Within WIMS10*, Proc. International Conference on the Physics of Reactors "Nuclear Power: A Sustainable Resource", Interlaken, Switzerland (September 2008)
- [25] E. Rutherford, *The scattering of  $\alpha$  and  $\beta$  particles by matter and the structure of the atom*. Phil. Mag., **21** (1911) 669–688. <https://doi.org/10.1080/14786440508637080>
- [26] H. Bateman, *The solution of a system of differential equations occurring in the theory of radioactive transformations*. In Proc. Cambridge Philos. Soc., **15** (1910) 423–427.
- [27] J. Cetnar, *General solution of Bateman equations for nuclear transmutations*. Annals of Nuclear Energy, **33** (2006) 640-645. <https://doi.org/10.1016/j.anucene.2006.02.004>
- [28] J. Rowlands, M. Salvatores, W. Assal, A.F. Avery, *et al*, *The JEF-2.2 nuclear data library*, JEFF Report 17: OECD Nuclear Energy Agency, Apr. 2000.
- [29] Z. Hiezl, D.I. Hambley, C. Padovani, W.E.Lee, *Processing and microstructural characterization of a  $UO_2$ - based ceramic for disposal studies on spent AGR fuel*, J. Nucl. Mater., **456** (2015) 74-84. doi: 10.1016/j.jnucmat.2014.09.002.
- [30] R.W. Mills, B.M. Slingsby, J. Coleman, R. Collins, G. Holt, C. Metelko, Y. Schnellbach, *A simple method for estimating the major nuclide fractional fission rates within light water and advanced gas cooled reactors*, Nucl. Engin. Technol., **52** (2020) 2130-2137. doi:10.1016/j.net.2020.03.004.
- [31] W. Hume-Rothery, *The sizes of atoms in metallic crystals*, Physica, **15** (1949) 29-33. [https://doi.org/10.1016/0031-8914\(49\)90021-X](https://doi.org/10.1016/0031-8914(49)90021-X)
- [32] W. Hume-Rothery, *Atomic diameters, atomic volumes and solid solubility relations in alloys*, Acta Metallurgica, **14** (1966) 17-20. [https://doi.org/10.1016/0001-6160\(66\)90267-7](https://doi.org/10.1016/0001-6160(66)90267-7)
- [33] R. E. Watson, L. H. Bennett, *Hume-Rothery Parameters and Phases*, Encyclopedia of Materials: Science and Technology (Second Edition) (2001) 3843-3849. <https://doi.org/10.1016/B0-08-043152-6/00684-7>
- [34] Y. M. Zhang, S. Yang, J. R. G. Evans, *Revisiting Hume-Rothery's Rules with artificial neural networks*, Acta Materialia, **56** (2008) 1094-1105. <https://doi.org/10.1016/j.actamat.2007.10.059>
- [35] M. C. Gao, C. Zhang, P. Gao, F. Zhang, J. A. Hawk, *Thermodynamics of concentrated solid solution alloys*, Current Opinion in Solid State and Materials Science, **21** (2017) 238-251. <https://doi.org/10.1016/j.cossms.2017.08.001>
- [36] L. Vegard, *Die Konstitution der Mischkristalle und die Raumfüllung der Atome*. Zeitschrift Phys., **5** (1921) 17-26. <https://doi.org/10.1007/BF01349680>
- [37] C. Mieszczynski, C. Degueldre, G. Kuri, J. Bertsch, C.N. Borca, *Investigation of irradiated uranium-plutonium mixed oxide fuel by synchrotron based micro X-ray diffraction*, Progress in Nuclear Energy, **57** (2012) 130-137. <https://doi.org/10.1016/j.pnucene.2011.11.012>

- 
- [38] K. Johansson, L. Riekehr, S. Fritze, E. Lewin, *Multicomponent Hf-Nb-Ti-V-Zr nitride coatings by reactive magnetron sputter deposition*, Surf. Coat. Technol., 349 (2018) 529–539. <https://doi.org/10.1016/j.surfcoat.2018.06.030>
- [39] M. Lestari, M. Lusi, *A mixed molecular salt of lithium and sodium breaks the Hume-Rothery rules for solid solutions*, Chemical communications 16 (2019) . <https://doi.org/10.1039/c8cc09850f>
- [40] E. Lewin, *Multi-component and high-entropy nitride coatings—A promising field in need of a novel approach*, Journal of Applied Physics **127** (2020) 160901. <https://doi.org/10.1063/1.5144154>
- [41] R.D. Shannon, C.T. Prewitt, *Effective ionic radii in oxides and fluorides*, Acta Cryst., B25 (1454) (1969) 925-946. <http://dx.doi.org/10.1007/s13398-014-0173-7.2>
- [42] S. Teth, *A study of the promolecule radius of nitrides, oxides and sulphides and of the bond critical properties of electron density distribution in nitrides*, PhD Thesis, Virginia State University, (1996)
- [43] W.H. Baur, *Effective ionic radii in nitrides*, Crystal Reviews, 1 (1987) 59-83. <https://doi.org/10.1080/08893118708081679>
- [44] J. Gebhardt, A.M. Rappe, *Big data approach for effective ionic radii*, Computer Physics Communications, 237 (2019) 238-243 <https://doi.org/10.1016/j.cpc.2018.11.014>
- [45] L. Pauling, *The Nature of the Chemical Bond, Third Edition*, Cornell University Press, Ithaca, New York, 1960. ISBN-13: 978-0801403330
- [46] G. Brown, *The Inaccessible Earth: An integrated view to its structure and composition*. Springer Science & Business Media (2012) 88. ISBN 9789401115162
- [47] M.H. Bradbury, H.J. Matzke, *Self-diffusion of plutonium in high burn-up simulated (U,Pu)(C,N) and (U,Pu)N*, J. Nucl. Mater. 91 (1980) 13-22. [https://doi.org/10.1016/0022-3115\(80\)90027-6](https://doi.org/10.1016/0022-3115(80)90027-6)
- [48] F. Poineau, C.B. Yeaman, G.W.C. Silva, G.S. Cerefice, A.P. Sattelberger, K.R. Czerwinski. *X-ray absorption fine structure spectroscopic study of uranium nitrides*. J. Radioanal. Nucl. Chem., 292 (2012) 989-994. <https://doi.org/10.1007/s10967-011-1551-7>
- [49] Y. Suzuki, Y. Arai, *Thermophysical and thermodynamic properties of actinide mononitrides and their solid solutions*, J. Alloys & Compounds, 271–273 (1998) 577-582. [https://doi.org/10.1016/S0925-8388\(98\)00160-1](https://doi.org/10.1016/S0925-8388(98)00160-1)
- [50] Y. Suzuki, Y. Arai, T. Iwai, T. Ohmichi, *Lattice Parameter of UN-PuN Solid Solution*, J. Nucl. Sci. Technol., 28 (1991) 689-691.
- [51] G. C. Jain, C. Ganguly, *Experimental evaluation of oxygen solubility in UN, PuN and (U,Pu) N*, J. Nucl. Mater., 202 (1993) 245-251. [https://doi.org/10.1016/0022-3115\(93\)90394-E](https://doi.org/10.1016/0022-3115(93)90394-E)
- [52] Y. Akimoto, *A Note on AmN and AmO*, J. Inorg. Nucl. Chem., 29 (1967) 136. [https://doi.org/10.1016/0022-1902\(67\)80191-X](https://doi.org/10.1016/0022-1902(67)80191-X)
- [53] H. Tagawa, *Phase Behavior and Crystal Structure of Actinide Nitrides*, Nippon Genshirvoku Gakkaishi, 5 (1971) 267.
- [54] J. P. Charvillat, U. Benedict, D. Darraen, Ch. de Novion, A. Wojakowski, W. Muller, *Preparation and Lattice Parameters of Actinide Monochalcogenides and Monopnictides, in Transplutonium Elements*, Proceedings of the 4th International Symposium, Baden-Baden, Sept. 13-

---

17, 1975, W. Muller and R. Lindner (Eds.), North-Holland Publishing Company, Amsterdam, 1976 138.

[55] M. Takano, H. Hayashi, K. Minato, *Thermal expansion and self-irradiation damage in curium nitride lattice*, J. Nucl. Mater., 448 (2014) 66-71. <https://doi.org/10.1016/j.jnucmat.2014.01.042>

[56] F. Natali, B.J. Ruck, N.O.V. Plank, H.J. Trodahl, S. Granville, C. Meyer, W.R.L. Lambrecht, *Rare-earth mononitrides*, Progress Mater. Sci., 58 (2013) 1316-1360. <https://doi.org/10.1016/j.pmatsci.2013.06.002>

[57] R.C. Brown, N.J. Clar, *The cerium-nitrogen-oxygen system. Oxygen as a component in the "binary" Ce-N system at 950°C*, Mater. Res. Bull., 9 (1974) 1007-1015. [https://doi.org/10.1016/0025-5408\(74\)90182-2](https://doi.org/10.1016/0025-5408(74)90182-2)

[58] Ch. P. Kempter, N. H. Krikorian, J. C. McGuire, *The Crystal Structure of Yttrium Nitride*, J. Phys. Chem., 61 (1957) 1237-1238. <https://doi.org/10.1021/j150555a023>

[59] A Zerr, G Miede, R Riedel, *Synthesis of cubic zirconium and hafnium nitride having Th<sub>3</sub>P<sub>4</sub> structure*, Nature materials, 2 (2003) 185-189. <https://doi.org/10.1038/nmat836>.

[60] R. W. Harrison, W. E. Lee, *Processing and properties of ZrC, ZrN and ZrCN ceramics: a review*, Advances in Applied Ceramics, 115 (2016) 294-307. <https://doi.org/10.1179/1743676115Y.0000000061>

[61] D.T. Olive, H. Ganegoda, T. Allen, Y. Yang, J. Terry. *Using a spherical crystallite model with vacancies to relate local atomic structure to irradiation defects in ZrC and ZrN*. J. Nucl. Mater., 475 (2016) 123-131. <https://doi.org/10.1016/j.jnucmat.2016.04.004>

[62] G. Brauer, R. Esselborn, *Nitridphasen des Niobs*, Z. anorg allg. Chem., 309 (1961) 151. <https://doi.org/10.10>

[63] D. Machon, D. Daisenberger, E. Soignard, G. Shen, T. Kawashima, E. Takayama-Muromachi, P.F. McMillan, *High pressure-high temperature studies and reactivity of  $\gamma$ -Mo<sub>2</sub>N and  $\delta$ -MoN*. Phys. Status Solidi A, 203 (2006) 831–836. <https://doi.org/10.1002/pssa.200521008>

[64] G. Linker, R. Smithey, O. Meyer, *Superconductivity in MoN films with NaCl structure*. J. Phys. F Met. Phys., 14 (1984) L115–L119. <https://doi.org/10.1088/0305-4608/14/7/005>

[65] Z. L. Zhao, K. Bao, D. F. Duan, X. L. Jin, F. B. Tian, D. Li, B. B. Liu, T. Cui, *Stoichiometric technetium nitrides under pressure: a first-principles study*. Сверхтвёрдые материалы, (super hard materials) 4 (2014) 89-98.

[66] K. Czerwinski, E. Mausolf, F. Poineau, D. Kolman, Th. Hartmann, Ph. Weck, G. Jarvinen, *Synthesis and characterization of technetium waste forms from an advanced fuel cycle*, Nuclear Medicine and Biology, 37 (2010) 686-687. <https://doi.org/10.1016/j.nucmedbio.2010.04.023>.

[67] Y. Zhang, L. Wu, B. Wan, Y. Lin, Q. Hu, *et al* . *Diverse ruthenium nitrides stabilized under pressure: a theoretical prediction*. Scientific reports (2016) 6 on line. <https://doi.org/10.1038/srep33506>

[68] M.G. Moreno Armenta, J. Diaz, A. Martinez-Ruis, G. Soto, *Synthesis of cubic ruthenium nitride by reactive pulsed laser ablation*, J. Phys. Chem. Solids, 68 (2007) 1989-1994. <https://doi.org/10.1016/j.jpcs.2007.06.002>



- 
- [69] R. Du, B. Suo, H. Han, Y. Lei, G. Zhai, *Theoretical study of electronic structure of rhodium mononitride and interpretation of experimental spectra*, Intern. J. Quantum Chem., 113 (2013) 2464-2470. <https://doi.org/10.1002/qua.24484>
- [70] J. C. Crowhurst, A. F. Goncharov, B. Sadigh, J.M. Zaug, D. Aberg, Yue Meng, V. B. Prakapenka, *Synthesis and characterization of nitrides of iridium and palladium*, J. Mater. Res., 23 (2008) 1-5. <https://doi.org/10.1557/JMR.2008.0027>
- [71] W. Martinsen, H. Warlimont, *Handbook of Condensed Matter and Materials Data*, Springer (2005)
- [72] U. Benedict, *The solubility of solid fission products in carbides and nitrides of uranium and plutonium, Part I: Literature review on experimental results*, Euratom Report EUR-5766 e, 1977; Part II: Solubility rules based on lattice parameter differences, Euratom Report EUR-5766 EN, 1977.
- [73] T.Song, Q.Ma, X.W.Sun, Z.J.Liu, Z.J.Fu, X.P.Wei, T.Wang, J.H.Tian, *Phase stability, electronic structure and equation of state of cubic TcN from first-principles calculations* Physics Letters A, 380 (2016) 3144-3148. <https://doi.org/10.1016/j.physleta.2016.07.040>
- 
- [74] D. H. Gregory, *Nitride chemistry of the s-block elements*, Coordination Chem. Rev., 215 (2001) 301-345. [https://doi.org/10.1016/S0010-8545\(01\)00320-4](https://doi.org/10.1016/S0010-8545(01)00320-4)
- [75] Feng Peng, Yunxia Han, Hanyu Liu, Yansun Yao, *Exotic stable cesium polynitrides at high pressure*, Sci. Rep., 5 (2015) 16902. <https://doi.org/10.1038/srep16902>
- [76] P. Ehrlich. *Calcium, Strontium, Barium Nitrides Ca<sub>3</sub>N<sub>2</sub>, Sr<sub>3</sub>N<sub>2</sub>, Ba<sub>3</sub>N<sub>2</sub>* in Handbook of Preparative Inorganic Chemistry, 2nd Ed. Edited by G. Brauer, Academic Press, NY, 1 (1963) 940-941.
- [77] J. H. Levy, J. C. Taylor, P. W. Wilson, *The structure of uranium tribromide by neutron diffraction profile analysis*, Journal of the Less Common Metals, 39 (1975) 265-270. [https://doi.org/10.1016/0022-5088\(75\)90200-3](https://doi.org/10.1016/0022-5088(75)90200-3)
- [78] A. Murasik, P. Fisher, W. Szczepaniak, *Neutron diffraction study of long-range antiferromagnetic order and crystal structure of uranium (III) tri-iodide*, J. Phys. C., Solid State Phys., 14 (1981) 1847
- [79] L.K.Matson, J.W.Moody, R.C.Himes, *Preparation and properties of some uranium selenides and tellurides*, Journal of Inorganic and Nuclear Chemistry 25 (1963) 795-800. [https://doi.org/10.1016/0022-1902\(63\)80364-4](https://doi.org/10.1016/0022-1902(63)80364-4)
- [80] O.L.Kruger, J.B.Moser, *Lattice constants and melting points of actinide-group IVA-VIA compounds with NaCl-type structures*, Journal of Physics and Chemistry of Solids, 28 (1967), 2321-2325 [https://doi.org/10.1016/0022-3697\(67\)90257-0](https://doi.org/10.1016/0022-3697(67)90257-0)
- [81] J. I. Grenthe, J. Drożdżyński, T. Fujino, E. C. Buck, T. E. Albrecht-Schmitt, S. F. Wolf, *Uranium*, Chap 5 in The Chemistry of the Actinides and Transactinides Elements edited by L. R. Morss, N. M. Edelstein, J. Fuger, Springer (2006)
- [82] W. Suski, A. Wojakowski, A. Blaise, P. Salmon, J.M. Fournier, T. Mydlarz, *Magnetic properties of the uranium sesquichalcogenides*, Journal of Magnetism and Magnetic Materials, 3 (1976) 195-200. [https://doi.org/10.1016/0304-8853\(76\)90032-9](https://doi.org/10.1016/0304-8853(76)90032-9)
- [83] O. Tougait, G. André, F. Bourée, H. Noël, *Neutron diffraction study of magnetic ordering of two binary uranium tellurides U<sub>3</sub>Te<sub>5</sub> and U<sub>2</sub>Te<sub>3</sub>*, Journal of Alloys and Compounds, 317-318, (2001) 227-232. [https://doi.org/10.1016/S0925-8388\(00\)01333-5](https://doi.org/10.1016/S0925-8388(00)01333-5)

- 
- [84] A. Salamat, K. Woodhead, S. Imran, U. Shah, A. L. Hector, P. F. McMillan, *Synthesis of  $U_3Se_5$  and  $U_3Te_5$  type polymorphs of  $Ta_3N_5$  by combining high pressure-temperature pathways with a chemical precursor approach*. Chem. Commun. 50, 10041–10044 (2014).  
<https://doi.org/10.1039/c4cc05147e>
- [85] P Böttcher, *Synthesis and crystal structure of  $Rb_2Te_3$  and  $Cs_2Te_3$* , Journal of the Less Common Metals, 70 (1980) 263-271 [https://doi.org/10.1016/0022-5088\(80\)90235-0](https://doi.org/10.1016/0022-5088(80)90235-0)
- [86] A.C. Sutorik, M.G. Kanatzidis, *Synthesis of  $[U(Se_2)_4]^{4-}$ : the first homoleptic actinide/polychalcogenide complex*, J. Am. Chem. Soc., 113 (1991) 7754-7755.  
<https://doi.org/10.1021/ja00020a043>
- [87] J. A. Cody, M. F. Mansuetto, J. A. Ibers, *New one-dimensional ternary and quaternary cesium-metal-tellurium compounds*. Journal of Alloys and Compounds, 219 (1995) 59-62.  
[https://doi.org/10.1016/0925-8388\(94\)05009-0](https://doi.org/10.1016/0925-8388(94)05009-0)
- [88] J.A. Cody, J.A. Ibers, *Uranium tellurides: new one- and two-dimensional compounds  $CsUTe_6$ ,  $CsTiUTe_5$ ,  $Cs_8Hf_5UTE_{30.6}$ , and  $CsCuUTe_3$* , Inorg. Chem., 34 (1995) 3165-3172.  
<https://doi.org/10.1021/ic00116a006>
- [89] G. N. Oh, J. A. Ibers, *Synthesis, structure, and electrical resistivity of  $Cs_3U_{18}Se_{38}$*  Journal of Solid State Chemistry, 192 (2012) 81-86. <https://doi.org/10.1016/j.jssc.2012.02.035>
- [90] D Gregory, M Barker, P Edwards, D. Siddons, *Synthesis and Structure of Two New Layered Ternary Nitrides,  $SrZrN_2$  and  $SrHfN_2$* , Inorg. Chem., 35 (1996) 7608-7613.  
<https://doi.org/10.1021/ic9607649>
- [91] A. Bowman, R. I. Smith, D. H. Gregory, *Synthesis and Structure of the Ternary and Quaternary Strontium Nitride Halides,  $Sr_2N(X, X')$  ( $X, X'$ : Cl, Br, I)*, Chem. Inform. 179 (2006) 130-139.  
<https://doi.org/10.1002/chin.200616003>.
- [92] A. S. Bailey, D. H. Gregory, P. Hubberstey, C. Wilson, *Crystal growth and redetermination of strontium nitride iodide,  $Sr_2NI$* , Acta Crystallographica E, 63 (2007). i177.  
<https://doi.org/10.1107/S1600536807039797>
- [93] Hj. Mattausch, R.K. Kremer, A. Simon, *Synthesis, Crystal Structure, and Magnetic Properties of  $Ce_{15}N_7I_{24}$* , ChemInform, 27(2010). <https://doi.org/10.1002/chin.199629009>
- [94] F. Lissner, Th. Schleid,  *$Ce_3NSe_3$ : Ein Cer(III)-Nitridselenid mit eckenverknüpften  $[NCe_4]^{9+}$ -Tetraedern*, Z. Anorg. Allg. Chem., 630 (2004) 1741. <https://doi.org/10.1002/zaac.200470096>
- [95] F. Lissner, Th. Schleid, *Die nicht-isotypen Nitridselenide  $Dy_3NSe_3$  und  $Ho_3NSe_3$ : Ketten und Dimere*, Z. Anorg. Allg. Chem., 635 (2009) 815-821. <https://doi.org/10.1002/zaac.200900005>
- [96] C. M. Schurz, P. Talmon-Gros, T. Schleid, *The gadolinium nitride selenides  $Gd_3NSe_3$  and  $Gd_{23}N_5Se_{27}$ : Three connectivity types of  $[NGd_4]^{9+}$  tetrahedra and fivefold coordinated  $Gd^{3+}$  cations*, Solid State Sciences, 17 (2013) 140-145. <https://doi.org/10.1016/j.solidstatesciences.2012.11.015>
- [97] F. Lissner, Th. Schleid,  *$Nd_4N_2Se_3$  and  $Tb_4N_2Se_3$ : Two non-isotypical lanthanide(III) nitride selenides*, ChemInform 34 (2003). <https://doi.org/10.1002/chin.200333013>
- [98] F. Lissner, Th. Schleid,  *$Pr_4N_2S_3$  und  $Pr_4N_2Se_3$ : Zwei nicht -isotype Praseodym(III)-Nitridchalcogenide*, Z. Anorg. Allg. Chem., 631 (2005) 427-432.  
<https://doi.org/10.1002/zaac.200400347>

- 
- [99] C.M. Schurz, Th. Schleid, *Dimorphic Ce<sub>4</sub>N<sub>2</sub>Se<sub>3</sub> with Orthorhombic Ce<sub>4</sub>N<sub>2</sub>Te<sub>3</sub>- and Monoclinic Nd<sub>4</sub>N<sub>2</sub>Se<sub>3</sub>-Type Structure*, Z. Kristallogr (Suppl. 31) (2012) 92- 104
- [100] F. Lissner, Th. Schleid, *Ln<sub>4</sub>N<sub>2</sub>Te<sub>3</sub> (Ln: La—Nd): The First Nitride Tellurides with Trivalent Lanthanides*, ChemInform, 36 (2005). <https://doi.org/10.1002/chin.200530024>
- [101] F. Lissner, O. Janka, Th. Schleid, *Pr<sub>5</sub>NSe<sub>6</sub>: Ein N<sup>3-</sup>-armes Praseodym(III)-Nitridselenid mit isolierten [N<sub>2</sub>Pr<sub>6</sub>]<sup>12+</sup>-Tetraederdoppeln gemäß [N<sub>2</sub>Pr<sub>6</sub>]Pr<sub>4</sub>Se<sub>12</sub>*, Z. Kristallogr (Suppl. 22) (2005), p. 166
- [102] C.M. Schurz, F. Lissner, O. Janka, Th. Schleid, *Synthese und Kristallstruktur der N<sup>3-</sup>-armen Nitridselenide des Formeltyps M<sub>5</sub>NSe<sub>6</sub> (M = La - Pr) mit isolierten Tetraederdoppeln [N<sub>2</sub>M<sub>6</sub>]<sup>12+</sup>*, Z. Anorg. Allg. Chem., 637 (2011) 1045-1051. <https://doi.org/10.1002/zaac.201100033>
- [103] Y. Dong, F. J. DiSalvo, *Ce<sub>2</sub>SeN<sub>2</sub>: Ternary selenide nitride containing tetravalent Ce in the Ce<sub>2</sub>SO<sub>2</sub> structure type*, Solid State Sciences, 13 (2011) 19-22. <https://doi.org/10.1016/j.solidstatesciences.2010.09.021>
- [104] P. C. H. Mitchell, T. Outteridge, K. Kloska, S. McMahon, Y. Epshteyn, R. F. Sebenik, A. R. Burkin, R.R. Dorfer, J.M. Laferty, G. Leichtfried, H. Meyer-Grünow, M.S. Vukasovich, *Molybdenum and molybdenum compounds*, (2020) Wiley on line.
- [105] A.E. Himri, M.E. Himri, D.P. Pérez-Coll, P. N. Núñez, *Co-precipitate precursor-based synthesis of new interstitial niobium molybdenum nitrides*, Res. Chem. Intermed., 41 (2015) 6397-6407. <https://doi.org/10.1007/s11164-014-1749-8>
- [106] B. Cordero, V. Gómez, A.E. Platero-Prats, M. Revés, J. Echeverría, E. Cremades, F. Barragán, S. Alvarez, *Covalent radii revisited*, Dalton Transactions, 21 (2008) 2832-2838. <https://doi.org/10.1039/B801115J>
- [107] R. Rajeswarapalanichamy, G. Sudha Priyanga, M. Kavitha, S. Puvaneswari, K. Iyakutti, *Structural stability, electronic structure and mechanical properties of 4d transition metal nitrides TMN (TM=Ru, Rh, Pd)*, J. Phys. Chem. Solids, 75 (2014) 888-902. <https://doi.org/10.1016/j.jpcs.2014.03.012>
- [108] H. Renner, G. Schlamp, I. Kleinwächter, E. Drost, H.M. Lüschof, P. Tews, P. Panster, M. Diehl, J. Lang, T. Kreuzer, A. Knödler, K.A. Starz, K. Dermann, J. Rothaut, R. Drieselman, R. (2002). *"Platinum group metals and compounds". Ullmann's Encyclopedia of Industrial Chemistry*. Wiley
- [109] D. C. Fee, C. E. Johnson, *Phase equilibria and melting point data for advanced fuel systems*, ANL report-AFP-10
- [110] M. Uno, K. Kurosaki, A. Nakamura, *Reactions of uranium nitride with platinum-family metals*, J. Nucl. Mater., 247 (1997) 322-327. [https://doi.org/10.1016/S0022-3115\(97\)00085-8](https://doi.org/10.1016/S0022-3115(97)00085-8)
- [111] S. Yamanaka, K. Yamada, T. Tsuzuki, T. Iguchi, M. Katsura, Y. Hoshino, W. Saiki, *Mechanical and thermal properties of uranium intermetallic compounds*, Journal of Alloys and Compounds, 271–273 (1998) 549-556. [https://doi.org/10.1016/S0925-8388\(98\)00152-2](https://doi.org/10.1016/S0925-8388(98)00152-2)
- [112] H. Yan, Yanqing Jiao, Aiping Wu, Chungui Tian, L. Wang, X. Zhang, H. Fu, *Synergism of molybdenum nitride and palladium for high-efficiency formic acid electrooxidation*. J. Mater. Chem. A, 6 (2018) 7623-7630. <https://doi.org/10.1039/C8TA02488J>

---

[113] C. Degueldre, C. Mieszczyński, C. Borca, D. Grolimund, J. Bertsch, *X-ray fluorescence and absorption analysis of krypton in irradiated nuclear fuel*, Nucl. Instrum. Meth. B, 336 (2014) 116-122. <https://doi.org/10.1016/j.nimb.2014.06.021>

[114] W.H. Keesom, H.H. Mooy, *The Crystal Structure of Krypton*, Nature, 125 (1930) 889. <https://doi.org/10.1038/125889a0>

[115] R. Sears, H.P. Klug, *Density and Expansivity of Solid Xenon*, J. Chem. Phys., 37 (1962) 3002-3006. <https://doi.org/10.1063/1.1733133>

[116] D. Zhou, J.H. Yu, Ch. Pu, Y. Song, *Prediction of Stable Ground-State Uranium Nitrides at Ambient and High Pressures*, arXiv March 2018. [https://doi.org/10.1016/0022-3115\(74\)90117-2](https://doi.org/10.1016/0022-3115(74)90117-2)